Desalination and Water Treatment
www.deswater.com
doi: 10.1080/19443994.2015.1128361

57 (2016) 21654–21663
September

Taylor & Francis
Taylor & Francis Group

Parametric, equilibrium, and kinetic study of the removal of salt ions from Ghanaian seawater by adsorption onto zeolite X

Bright Kwakye-Awuah[a,*], Elizabeth Von-Kiti[a], Isaac Nkrumah[a], Rose Erdoo Ikyreve[b], Iza Radecka[c], C. Williams[c]

[a]*Department of Physics (Materials Science Group), KNUST, University Post Office, Private Mail Bag, Kumasi, Ghana, Tel. +233 3220060 299; email: bkwakye-awuah.cos@knust.edu.gh (B. Kwakye-Awuah), Tel. +233 545207159, Tel. +233 242579383; email: vonliz05@yahoo.co.uk (E. Von-Kiti), Tel. +233 540987552; email: inkrumah.sci@knust.edu.gh (I. Nkrumah)*
[b]*Department of Chemistry, Benue State University, Markudi, Nigeria, Tel. +234 8036979663; email: erdoo_r@yahoo.com*
[c]*Faculty of Science and Engineering, University of Wolverhampton, WV1 1LY, Wolverhampton, United Kingdom, Tel. +44 1902322366; email: i.radecka@wlv.ac.uk (I. Radecka), Tel. +44 1902322159; email: c.williams@wlv.ac.uk (C. Williams)*

Received 29 September 2013; Accepted 12 November 2015

ABSTRACT

Zeolite X was synthesized in the laboratory and was characterized using X-ray diffraction, scanning electron microscopy, thermogravimetric analysis, energy dispersive X-ray spectrometer, and Fourier transformed infrared spectrometry. Desalination activity of zeolite X was investigated by the ion-exchange process. The pH of the seawater prior to desalination analysis was 7.87 ± 0.03 through the period of the investigation. The conductivity of the seawater was found to be 16.2 ± 0.01 mS/cm. Effect of time on ion removal was measured. Removal efficiencies of ions showed a trend of $Ca^{2+} > K^{+} > Mg^{2+} > Na^{+}$. Equilibrium data were fitted by Langmuir and Freundlich isotherms and parameters were evaluated using these models. Adsorption capacities obtained followed the order $Ca^{2+} > K^{+} > Mg^{2+} > Na^{+}$ with R^2 values $K^{+} > Na^{+} > Ca^{2+} > Mg^{2+}$ for both Langmuir and Freundlich parameters. Equilibrium kinetic data were analyzed using adsorption kinetic models: pseudo-first-order and pseudo-second-order kinetic models. A linear regression method was used to estimate the adsorption and kinetic parameters. The R^2 values obtained followed the order $K^{+} > Mg^{2+} > Ca^{2+} > Na^{+}$ for both pseudo-first- and pseudo-second-order kinetic models. Zeolite X has attractive features as an adsorbent for desalination of seawater.

Keywords: Desalination; Synthesis; Zeolite X; Seawater; Kinetics; Removal efficiency

1. Introduction

Seawater is an abundant natural resource. About 71% of the Earth's surface is covered by water which is in the form of oceans, seas, and ice at the poles [1,2]. However, only about 3% of the water is fresh and suitable for drinking. The water of the oceans and seas is salty and therefore not directly usable. There is at present permanently high growing need of fresh clean water by the world at large. Furthermore, due to population growth coupled with unpredicted droughts in Sub-Saharan Africa, water scarcity is gradually reaching alarming proportion. Hence, the need to find improved, economical, alternative source (s) of water has not only become desirable but also

*Corresponding author.

paramount [2,3]. In recent times, desalination techniques have been used to desalinate seawater, brackish water or wastewater resulting in significant achievements [1,4]. Desalination refers to several processes that remove excess salt and other minerals from water and usually involves a phase change such as freezing and distillation in thermal processes but also membranes in reverse osmosis and electrodialysis experiments [5–7]. To take advantage of natural resources, attention has been focused on desalination of seawater and brackish water, using effective however still expensive techniques [3,4,6,8]. However, high capital and energy are required, making the use of these techniques very expensive [4,7]. In recent years, zeolites have been considered as the best alternative to achieve high desalination rates with virtually no introduction of harmful chemicals while effectively removing cations and anions in varying ways [8,9]. Zeolites are crystalline hydrated aluminosilicates whose framework structure consists of cavities or pores that are occupied by cations and water molecules [10–17]. Both the cation and the water molecule have considerable freedom of movement permitting ion exchange and reversible dehydration [11–17]. There are over 40 known natural zeolites and 160 synthetic zeolites have been documented [10]. Synthetic zeolites have wider applications than natural zeolites due to their purity and also modification of the Si/Al ratio to suit a particular application [10,13]. Zeolite X is a synthetic counterpart of the naturally occurring mineral Faujasite and has one of the largest cavities and cavity entrances of any known zeolites [10,15,17]. In this work, zeolite X was synthesized in the laboratory and its desalination activity and efficiency on Ghanaian seawater was investigated. Equilibrium data were fitted by Langmuir and Freundlich isotherms and parameters were evaluated using these models. Equilibrium kinetic data were analyzed using adsorption kinetic models: pseudo-first-order and pseudo-second-order kinetic models and linear regression method were used to estimate the adsorption and kinetic parameters.

2. Materials and method

2.1. Materials and reagents

Seawater was obtained from Dansoman, a suburb of Accra, Ghana. Whatman filters no. 1 were purchased from Sigma–Aldrich, UK. Zeolite X was synthesized in the Water Research laboratory, KNUST and characterized in the School of Applied Sciences, Wolverhampton University UK. Ion chromatography (IC; ICS-1000, Dionex, USA) was available at the Chemistry Research laboratory, KNUST while inductively coupled plasma atomic emission spectrometer (ICP-AES; SPECTRO 2005, UK) was available at University of Wolverhampton, UK. Sodium hydroxide, sodium aluminate, and sodium metasilicate were purchased from Sigma Aldrich, UK. Distilled water was supplied by the Water Research group, KNUST. Sodium hydroxide, potassium hydroxide, aluminum oxide, and sodium silicate were purchased from Sigma Aldrich, UK.

2.2. Synthesis of zeolite X

Zeolite X was synthesized in the laboratory according to the method reported by Kwakye-Awuah et al. [17] with some modifications. The batch composition of the synthesis reaction was 0.18 NaOH: 0.1 Al_2O_3: 0.4 SiO_2: 32.4 H_2O. A mass of 7.2 g of sodium hydroxide (Sigma–Aldrich, UK) was added to 166 ml of deionized water in a plastic beaker while stirring until a homogeneous solution was obtained. A total of 10.2 g of alumina powder (Sigma Aldrich, UK) was then added and stirring was continued until a homogeneous slurry was obtained. The sodium aluminate suspension was added to 36.0 g of sodium silicate solution (Sigma–Aldrich, UK) to form a gel, while stirring until the gel was homogenized. The gel was poured into Teflon vessels. The bottles were put into an electric oven at a temperature of 100˚C for 6 h. The reaction in the Teflon bottles was quenched by running cold water on the bottles after they were removed from the oven until they were cooled to room temperature. The synthesized samples were filtered using a Buchner vacuum funnel and Whatman no. 1 filter paper. The powder samples obtained were washed copiously with 500 ml of distilled water. Following overnight drying of the powdered zeolite at 40˚C in an electrical oven, the zeolite was crushed into uniform powder with pestle and mortar, sieved and stored in a cupboard.

2.3. Characterization of zeolite X

To confirm the crystal structure and the composition of the synthesized zeolite, it was essential to characterize the zeolite. The X-ray diffraction (XRD) pattern of the zeolite X which gives a measure of phase purity were recorded on Phillips PW 1710 X-ray powder diffractometer over 2θ range of 3˚–50˚ (PANalytical, UK Ltd, Cambridge). The diffractometer was equipped with a graphite monochromated Cu K_α radiation source (8,987 eV; $\lambda = 1.5418$ Å) Data processing was carried out using Philips APD software with

a search/match facility and an ICDD database on a DEC Microvax minicomputer interfaced to the diffractometer. The surface morphology of the zeolite as well as the elemental composition were examined by scanning electron microscopy (SEM) using a Zeiss EVO 50 equipped with energy dispersive X-ray spectrometer (EDX) (Zeiss, UK). Aluminum stubs were prepared prior to the analysis with an adhesive coating. The samples were sprinkled on the stubs. Where necessary, the samples were gold-coated using an Emscope SC500 Sputter coater to reduce static charging. Electron micrographs were obtained at various magnifications.

Particle size distribution per unit volume was analyzed using a mastersizer long bed analyzer (Malvern Instruments, UK). Samples of silver-exchanged zeolite X were taken for particle size analysis. Before measurements were made the laser lenses were aligned in a straight line. Settings were set to obscuration value of 0.2. After steady conditions, 0.1 mg of each sample was loaded into an MSX 15 sample handling unit that uses the mechanical action of stirring to ensure that the zeolite particles did not flocculate. Sodium Amalgam was then added to disperse adhering particles. Measurements were then recorded on a computer connected to the instrument.

The vibrational properties were investigated by Fourier transformed infrared spectrometry (FTIR). Measurements were done using 100 scans at 4 cm^{-1} resolution, units of log(1/*T*) (absorbance), over the mid-IR region of 1,200–400 cm^{-1}. An air background spectrum was collected at the start of the sample analysis. A small sample of each zeolite was centered on the ZnSe plate to ensure that it covered the entire crystal surface, and a pressure clamp was used to apply pressure on the sample. The zeolite samples were analyzed three times for three different samples. A background spectrum was measured before every sample to compensate for atmospheric conditions around the FT-IR instrument. Thermogravimetric (TGA) analysis was performed using a Perkin Elmer TGA 7 (Perkin Elmer, UK). The temperature range for the analysis was 50–800 °C.

2.4. Desalination based on ion removal

2.4.1. Adsorption isotherm studies

Raw seawater samples from Dansoman Beach in Ghana were filtered using a fiber glass filter of 0.45-μm pore diameter to remove particulate matter. Adsorption capacity of ions in the seawater by zeolite X was studied using the batch technique. In a series of 250-ml Erlenmeyer flasks each containing 100 ml of Ghanaian seawater, 0.5 g of zeolite X was added. The flasks were capped and placed on a rotary shaker (200 rpm) at room temperature. The initial pH value of the seawater was 7.87. The investigated times were 15, 30, 60, 90, and 120 min. The zeolite was filtered out of the seawater after each allocated time. The final pH was measured. The concentrations of Na^+, K^+, Mg^{2+}, and Ca^{2+} ions were determined to ascertain the amount of ions adsorbed by the zeolite. The whole procedure was repeated twice to ascertain the reproducibility of the results.

3. Results and discussion

3.1. Characterization of zeolite X

The SEM micrographs (Fig. 1) showed cubic morphology of crystalline sample of zeolite X before and after addition to seawater. The mid-FTIR spectra of the as-synthesized zeolite X is given in Fig. 2 in the region of lattice vibrations (1,200–400 cm^{-1}). A large broad band was observed at 975 cm^{-1}. Other bands were observed at 790, 695, 585, and 450 cm^{-1}. This band can be attributed to the overlap of the asymmetric vibrations of Si–O (bridging) and Si–O^- (non-bridging) bonds. Symmetric stretching of the external T–O linkages occurred at 790 cm^{-1}, while the symmetric stretching due to the internal vibrations of the zeolite X framework tetrahedra occurred at 695 cm^{-1}. Vibrations associated with the double six rings (D6R) that connect the sodalite cages occurred at 585 cm^{-1}. The band at 450 cm^{-1} is assigned to the internal vibrations due to the bending of the T–O tetrahedra. [17,18]. The XRD pattern of zeolite X (Fig. 3) matches that of the literature, with a flat base and distinct peaks indicating a highly crystalline product with no impurities. All the peaks obtained matches that of the ICDD database for zeolite X. The purity of zeolite X was confirmed as there was no other phases or lines present. Significant peaks were noted at 2θ = 6°, 11°, 22°, 25°, and 29° [17,19–23]. Smaller peaks were also observed. Crystallinity observed could be attributed to the presence of Al in the starting gel [17]. This was confirmed by the TGA results (Fig. 4) which portrayed a highly stable zeolite. It was clear from the thermogravimetric analysis plot (Fig. 4) of zeolite X that the maximum weight loss of 5.8% was observed at 99 °C and this could probably be due to the removal of water on the surface. Further weight loss of approximately 7% occurred between 100 and 300 °C which can be attributed to the loss of water within the framework. EDX analysis showed that the composition of the synthesized zeolites were aluminosilicate in addition to sodium ions (Table 1).

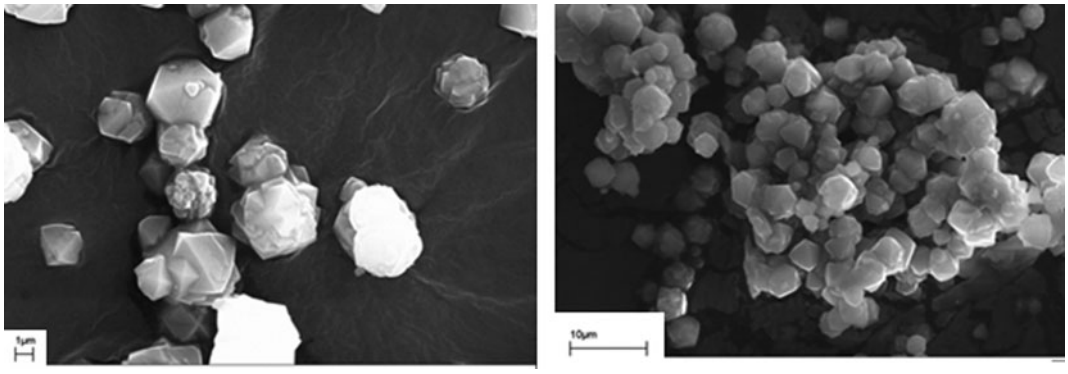

Fig. 1. SEM images showing the size of zeolite X crystals at different resolution.

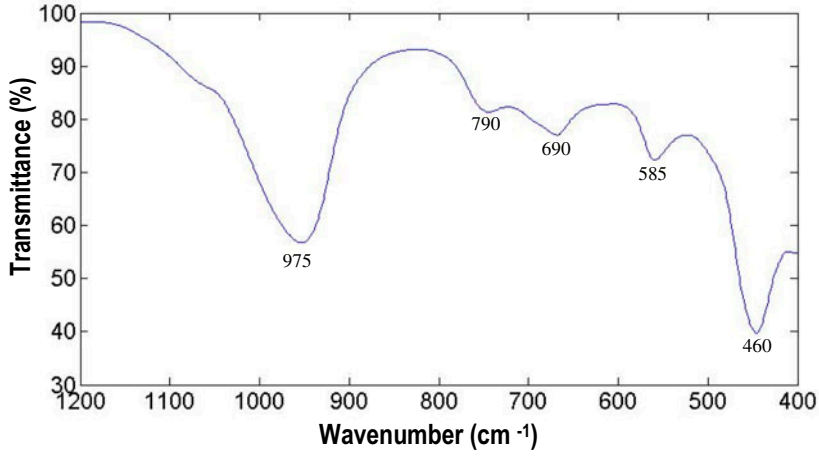

Fig. 2. FTIR spectrum of zeolite X.

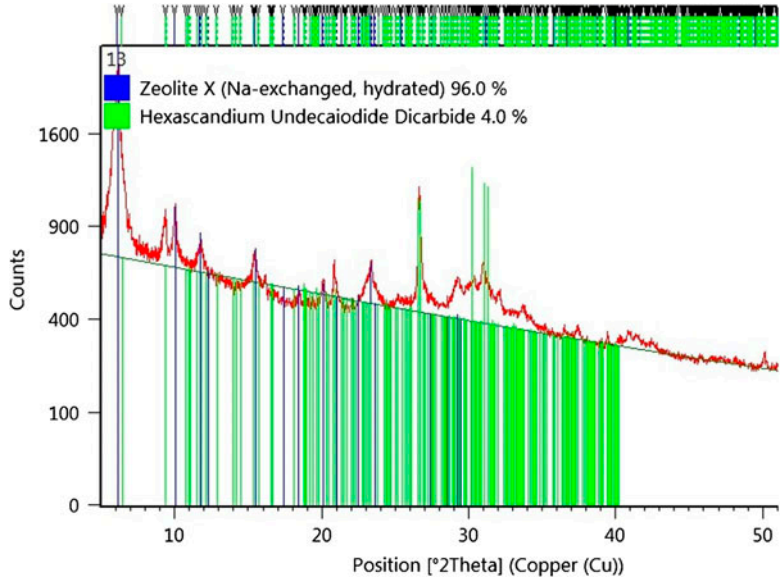

Fig. 3. XRD pattern of zeolite X showing peaks for $2\theta = 0^{\circ}$–50°.

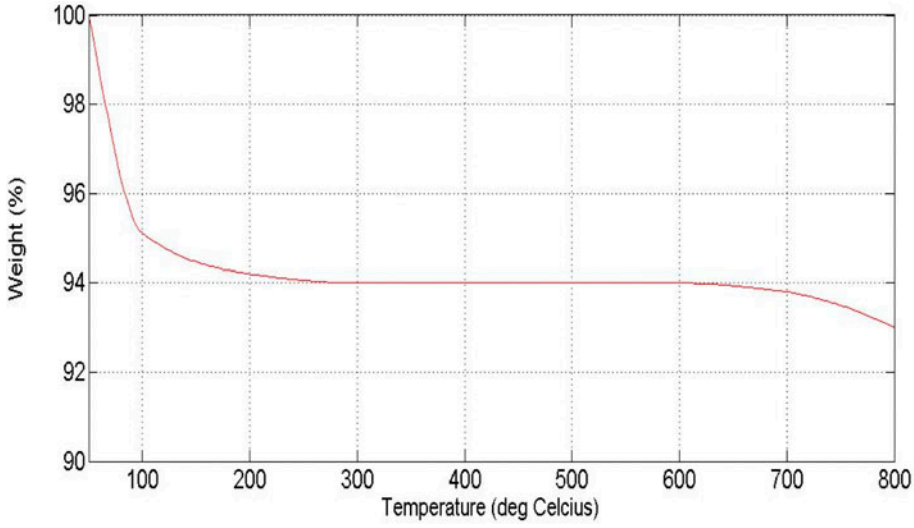

Fig. 4. Thermogravimetric analysis plot for zeolite X for temperature 50–800°C.

Table 1
Elemental composition of synthesized zeolite X

Element	wt.%
Na	5.3
Al	15.2
Si	22.6
O	56.9

3.2. Desalination activity and adsorption isotherms

3.2.1. Seawater composition, changes in pH and conductivity

The chemical composition of the pretreated water was evaluated by inductively coupled plasma atomic emission spectrometry (ICP; SPECTRO 2005, Siemens, UK) and ion chromatography (IC; ICS-1000, Dionex, USA). The seawater was diluted (10×) and the detection limit for all the measured ions was 0.1 ppm. In the chromatography analysis, the seawater was also diluted (10×) with detection limit for all measured ions as 0.05 ppm. Table 2 shows the salt concentrations of the filtrated seawater. The composition of the seawater is a typical one: $Cl^- >> Br^- >> Mg^{2+} \approx S > K^+ > Ca^{2+} > F^-$. Additionally, there were small detections of NO_3^- and PO_4^{3-} ions.

Changes in pH and electrical conductivity (EC) in mS/cm with time were also recorded. For this investigation, the ratio of zeolite mass (in grams) to volume of seawater (in ml) was 0.5:100. Temperature and other conditions were constant. A considerable increase in the pH of seawater was observed. The pH increased from 7.61 to 8.41 when zeolite X was added for 15 min. This effect is attributed to the pH of the synthesized zeolite (9.91) when introduced into the seawater causing a surge in the sample's overall pH. The pH after 30 min saw a further increase though not very high (0.03), and an additional increase of 0.01 after 60 min. Tests for portable drinking water include measuring pH, total hardness of raw and treated water, and chloride concentration. To improve the quality of seawater so as to bring the quality to drinking water standard, the concentrations of anions such as Cl^-, SO_4^{2-}, and NO_3^- were determined by titration. Following the results obtained (not shown) Cl^- concentration was higher than WHO recommended limit, whereas NO_3^- was far lower than the allowed limit set by WHO. Hence, Cl^- in the seawater was precipitated by adding 0.1 mM $AgNO_3$ to the seawater and

Table 2
Chemical composition of seawater after filtration process

		Concentration (ppm)	
Element	Chemical state in seawater	ICP-OES	IC
Na	Na^+	4,872	
K	K^+	1,075	
Mg	Mg^{2+}	1,141	
Ca	Ca^{2+}	758	
S	SO_4^{2-}	1002	3,540
N	NO_3^-		2.90
P	PO_4^{3-}		4.26
F	F^-		0.97
Cl	Cl^-		3,059
Br	Br^-		63.88

parameters such as pH, EC, and total dissolved solids (TDS) were again measured. The amount of chloride present was found to be 18.7 ppt.

The precipitation reaction equation for Na^+ and K^+ is presented by:

$$AgNO_{3(aq)} + XCl_{(aq)} \rightarrow AgCl_{(s)} + XNO_{3(aq)} \quad (1)$$

For Mg^{2+} and Ca^{2+} the reaction equation is:

$$AgNO_{3(aq)} + XCl_{2(aq)} \rightarrow AgCl_{2(s)} + XNO_{3(aq)} \quad (2)$$

Silver nitrate reacted with the chloride ions forming a white precipitate (silver chloride). The pH was monitored at regular intervals as with initial tests. By introducing silver nitrate into the sample, the pH and EC were considerably reduced. The pH was reduced by 0.97 ± 0.05. The EC was also reduced by 3.22 ± 0.4 mS/cm. Initial concentration of cations in seawater was: Na^+ = 4,782.40 ± 0.1 mg/l, K^+ = 1,789.05 ± 0.1 mg/l, Mg^{2+} = 828.13 ± 0.1 mg/l, Ca^{2+} = 751.75 ± 0.1 mg/l. The addition of zeolite X to the seawater saw an increment of 0.89 units to the pH within the first 15 min, while EC reduced further from 6.53 to 6.20. A reduction in concentration was observed in all four elements between 15 and 120 min except for Na^+ which leached at 120 min. Removal efficiencies showed a trend of for $Ca^{2+} > K^+ > Mg^{2+} > Na^+$.

3.2.2. Desalination and adsorption isotherms

The element removal efficiency, R % of ions was calculated using the formula:

$$R\,\% = \frac{C_i - C_f}{C_i} \times 100\% \quad (3)$$

where C_i is the concentration of elements in seawater before addition of zeolite X, and C_f is the concentration of elements after ion exchange with zeolite X.

In Fig. 5, it was observed that there was steady removal of Na^+ after 15 min of zeolite X to the seawater up to 60 min. Thereafter, there was a slight reduction in the removal efficiency at 90 min but later showed maximum efficiency at 120 min (32%). Similarly, the rate of removal of K^+ increased in the first 30 min but decreased at 60 min after which it showed steady removal with the highest removal of 58% at 120 min. Mg^{2+} was steadily removed up to 90 min but removal was reduced slightly at 120 min. A similar trend was observed for Ca^{2+} with highest removal of 81.5% at 90 min. This can be attributed to the fact that the synthesized zeolite X had no Ca^{2+} in its framework.

Zeolites selectivity related to cations and anions is an important property in water treatment procedures. Selectivity is a property of the exchanger to show different preferences for particular ions and it depends on the field strength in the zeolite pore. The higher removal of one ion over the other depends on the equilibrium state of the activity. The ion-exchange tests that were run showed an increase in the sloutions pH (hydrolysis of zeolites) (Table 3). This occurrence is due to the removal of calcium and magnesium and its replacement by sodium ions present in the zeolite framework [24–28]. It was not possible to achieve complete ion exchange of cations, especially K^+ with Na^+. This was because of Na cations in the zeolite framework. However, as stated by Barrer [10], K^+ is still preferred in the Faujasite framework over Na^+. Therefore, the selectivity for K^+ over Na^+ is smaller in the higher charged zeolite than in the lower charged ones. The study showed that selectivity of ions by low silica zeolite X was found to be higher for divalent cations than for monovalent cations. Sherman [28] in his work stated a selectivity of $K^+ > Na^+$ and $Ca^{2+} > Mg^{2+}$. In this work, however, the order of selectivity for cations observed was $Ca^{2+} > Mg^{2+} > K^+ > Na^+$. This order of selectivity could be attributed to the fact that zeolites prefer ions

Table 3
pH and conductivity of seawater obtained for each sampling time

	pH		Conductivity (mS/cm)		TDS	
Time (min)	Seawater + Z-X	Seawater + Z-X + $AgNO_3$	Seawater + Z-X	Seawater + Z-X + $AgNO_3$	Seawater + Z-X	Seawater + Z-X + $AgNO_3$
0	7.61 ± 0.02	7.38 ± 0.02	16.70 ± 0.02	6.53 ± 0.01	4,876 ± 0.01	4,875 ± 0.02
15	8.41 ± 0.03	7.30 ± 0.03	15.55 ± 0.02	6.2 ± 0.01	4,679 ± 0.01	3,100 ± 0.03
30	8.44 ± 0.04	7.38 ± 0.03	15.00 ± 0.03	6.08 ± 0.02	4,435 ± 0.02	3,040 ± 0.02
60	8.45 ± 0.03	7.72 ± 0.02	13.51 ± 0.02	6.02 ± 0.01	4,304 ± 0.01	3,010 ± 0.03
90	8.43 ± 0.03	7.70 ± 0.03	11.00 ± 0.03	5.91 ± 0.02	4,210 ± 0.02	2,955 ± 0.02
120	8.48 ± 0.02	7.58 ± 0.01	10.69 ± 0.03	6.09 ± 0.02	4,152 ± 0.02	3,045 ± 0.02

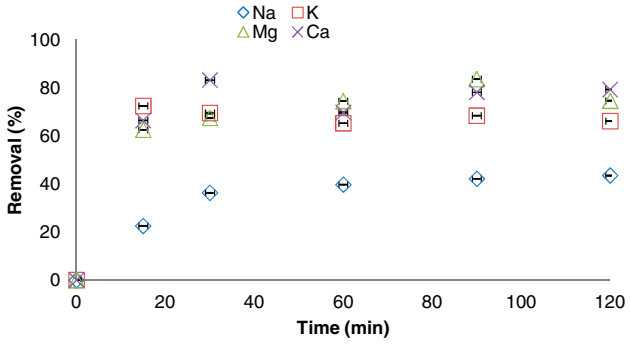

Fig. 5. Graph showing the average removal efficiencies with standard deviations of the various cations. The experiment was repeated three times and results averaged.

of higher charge [25,29]. In the same light, Kuronen et al. [24] stated that highly aluminous zeolites are known to be selective to divalent cations. It was reported in their study that a higher selectivity for Sr^{2+} than K^+ in ion exchange with Na^+ in MAX (maximum aluminum zeolite X) was observed. The preferred counter ion was taken up by the exchanger at a higher relative rate. The presence of Ca^{2+} and Mg^{2+} in the seawater influence the uptake of K^+ and Na^+ [25]. The process of cation uptake by zeolites is determined by the kinetics of adsorption. The amount of Na^+ released into the seawater by zeolites indicates ion-exchange activity. Since there was sodium in both seawater and zeolite, the effective removal of all cations was hindered. Very often, a zeolite favors the least hydrated ion, while the solution phase favors the most hydrated ion [25,27]. The effect of competitive cations and anions on ion exchange of heavy metals in clinoptilolite was examined by Inglezakis et al. [27]. The presence of cations in the solution of the heavy metals is reducing the presence of the latter due to simultaneous exchange of cations which occupy available exchange sites in the zeolite structure. Furthermore, the results indicate that zeolite X has a high capacity for removing Ca^{2+} and Mg^{2+} ions as time progressed. Thus, the initial 15 min favored the adsorption of Ca^{2+}, Mg^{2+}, and K^+, whereas Na^+ was either excluded due to its size/or charge. In reality, more than one model is required to correlate adsorption equilibrium since there is no universal equilibrium model that provides an accurate fit for all adsorption isotherms [26,30]. Thus, three typical adsorption models were applied in this study to fit the adsorption isotherms for the four ions (sodium, potassium, magnesium, and calcium) in an attempt to obtain the optimum model by the comparison of accuracy of the models. Adsorption equilibrium data were analyzed using the Langmuir, Freundlich, and Langmuir–Freundlich isotherm models. The Langmuir isotherm theory assumes monolayer coverage of adsorbate over a homogeneous adsorbent surface. This implies that all adsorbing sites are equivalent and adsorption on an active site is independent of whether or not an adjacent site is occupied. Mathematically, the model is given by the equation [30]:

$$q_e = \left(\frac{Mk_L}{1 + k_L C_e}\right) \tag{4}$$

where C_e (mg/L) is the equilibrium concentration, q_e (mg/g) is the amount of salt ion adsorbed at equilibrium, M (mg/g) and k_L (L/mg) are the maximum adsorption capacity and Langmuir constants, respectively.

The linearized form can be express as:

$$\frac{C_e}{q_e} = \frac{1}{Mk_L} + \frac{C_e}{M} \tag{5}$$

The values of M and k_L were calculated from the slope and intercept of the plot of C_e/q_e as ordinate and C_e as abscissa. Results obtained for Langmuir adsorption parameters are shown in Table 4. The Freundlich isotherm assumes a multilayer adsorption with interactions between ions and is expressed as [30]:

$$q_e = k_F C_e^{\frac{1}{n}} \tag{6}$$

where q_e (mg/g) is the amount of ammonium ion adsorbed at equilibrium, k_F (measure of adsorption capacity) and $1/n$ (measure of adsorption intensity) are Freundlich constants. Taking natural log on both sides of Eq. (6), we obtain:

$$\ln q_e = \ln k_F + \frac{1}{n} \ln C_e \tag{7}$$

Values of C_e and k_F are calculated from a plot of $\ln q_e$ as ordinate and $\ln C_e$ as abscissa and are given in Table 4. It can be seen that the value of $R^2 \geq 0.90$ for all cases indicate that both Langmuir and Freundlich equations well fitted the adsorption isotherm. Furthermore, the inverse of the Freundlich coefficient n is less than one, confirming that adsorption is favorable. In addition, the Langmuir and Freundlich constants obtained were well within experimental adsorption data. Thus, both Langmuir and Freundlich models predicted correctly the equilibrium adsorption isotherms for all the ions by zeolite X. The coefficient

Table 4
Adsorption Isotherm equation coefficients extracted from the plot of linearized curves (not shown)

Ion	Model used					
	Langmuir parameter			Freundlich parameter		
	M (mg/g)	k_L (l/mg)	R^2	k_F (mg/g)	N	R^2
Na	0.06	0.633	0.901	1.203	2.102	0.911
K	0.2	3.867	0.986	2.371	2.527	0.971
Mg	0.1	20.613	0.956	1.103	2.8609	0.932
Ca	0.1	38.195	0.942	1.078	4.548	0.913

Table 5
Adsorption Isotherm equation coefficients extracted from the linearized

	Model used							
	Pseudo-first-order nonlinear				Pseudo-second-order nonlinear			
Ion	k_1 (l/min)	$q_{e,exp}$ (mg/g)	$q_{e,calc}$ (mg/g)	R^2	k_2 (l/min)	$q_{e,exp}$ (mg/g)	$q_{e,calc}$ (mg/g)	R^2
Na	0.3560	38.89000	40.46753	0.93830	9,166.7	16,508.0	1,666.7	0.991
K	0.3580	20.78000	21.03526	0.95990	322.2	323.2	333.3	0.999
Mg	0.1280	33.26000	33.64283	0.92020	177.5	764.4	769.2	0.989
Ca	0.570	19.34000	19.58375	0.79450	21.6	238.9	232.6	0.994

of determination R^2 below 0.93 indicated that the modeling performance of Freundlich equation for Na^+ and Ca^{2+} were slightly inferior to that of Langmuir model ($R^2 \geq 0.94$).

3.3. Kinetic studies

To understand the adsorption mechanism of salt ion uptake onto zeolite X at time t, the pseudo-first- and second-order kinetic models were used. Pseudo-first-order kinetic model is given by the equation [30]:

$$\frac{dq_t}{dt} = k_1(q_e - q_t) \tag{8}$$

Integrating (5) from $t = 0$ to $t = t$ and from $q_t = 0$ to $q_t = q_t$, we obtain:

$$\ln(q_e - q_t) = \ln q_e + k_1 t \tag{9}$$

where q_e (mg/g) and q_t (mg/g) are the amount of salt ion adsorbed at equilibrium and at time t and k_1 (1/min) is the pseudo-first-order rate constant. The values of q_e and k_1 were calculated from the slope and intercept of a plot of $\ln(q_e - q_t)$ as ordinate and t as abscissa. Table 5 shows that the experimental value obtained for q_e is far greater than that obtained from calculation. Furthermore, the R^2 value obtained suggests that the experimental data did not fit the pseudo-first-order kinetic model. The pseudo-second-order kinetic model is given by the expression [30]:

$$\frac{dq_t}{dt} = k_1(q_e - q_t)^2 \tag{10}$$

Integrating from $t = 0$ to $t = t$ and from $q_t = 0$ to $q_t = q_t$, we obtain:

$$q_t = \frac{t}{\frac{1}{k_2 q_e^2} + \frac{t}{q_e}} \tag{11}$$

where again, q_e (mg/g) and q_t (mg/g) are the amount of salt ion adsorbed at equilibrium and at time t and k_2 (1/min) is the pseudo-first-order rate constant. The values of q_e and k_1 were calculated from the slope and intercept of a plot of t/q_t as ordinate and t as abscissa. Results obtained are shown in Table 5. As can be seen from Table 5, the R^2 values obtained showed high correlation. Furthermore, the experimental and theoretical values of q_e and q_t are in good agreement. It therefore follows that pseudo-second-order kinetics predominates compared with pseudo-first-order kinetics. Thus,

the rate-limiting step is likely to be chemical sorption, involving forces through the sharing of or exchange of electrons between the adsorbent and the adsorbate.

4. Conclusion

According to the results, cation-exchange behavior of zeolite X showed a good selectivity for calcium and poor selectivity for sodium. Different zeolite ratios reported similar trends. Selectivity is higher for divalent cations than for monovalent cations in zeolite X. The selectivity sequence was determined as Ca > Mg > K > Na. Poor selectivity for Na could be explained as due to the presence of Na in the framework through synthesis. The quality of water produced was high in Na^+ making it unsuitable for drinking. However, it is worth mentioning that retrieval of the zeolite and addition of fresh zeolite was likely to have reduced the Na^+ to drinking water quality. The levels of Ca^{2+} and Mg^{2+} were well below the allowed limit for drinking water as recommended by WHO [31]. Langmuir and Freundlich isotherms both demonstrated to provide good fit for the sorption of salt ions onto zeolite X. The adsorption capacity of zeolite X was found to be 72.99 and 72.46 mg/g for first addition and retrieval and 71.94 for second and third retrieval process. Kinetics studies suggest that salt ion adsorption on zeolite X could be described more favorably by the pseudo-second-order model with the parameters better estimated by the linear method. Finally, it can also be concluded that zeolite X has the attractive features of being a good adsorbent for desalination of seawater.

References

[1] M.C. Duke, J. O'Brien-Abraham, N. Milne, B. Zhu, J.Y.S. Lin, J.C.D. de Costa, Seawater desalination performance of MFI type membranes made by secondary growth, Sep. Purif. Technol. 68 (2009) 343–350.
[2] C.H. Cho, C.K.Y. Oh, S.K. Kim, J.G. Yeo, P. Sharma, Pervaporative seawater desalination using NaA zeolite membrane: Mechanisms of high water flux and high salt rejection, J. Membr. Sci. 371 (2011) 226–238.
[3] A. Al-Ansari, H. Ettouney, H. El-Dessouky, Water-zeolite adsorption heat pump combined with single effect evaporation desalination process, Renewable Energy 24 (2001) 91–111.
[4] M.C. Duke, S. Mee, J.C.D. de Costa, Performance of porous inorganic membranes in non-osmotic desalination, Water Res. 41 (2007) 3998–4004.
[5] E. Brauns, V. Van Hoof, C. Dotremont, H. De Wever, P. Lens, E. Van Hoof, G. Thomas, B. Molenbergh, D. DeMey, The desalination of an *Arthrospira platensis* feed solution by electrodialysis and reverse osmosis, Desalination 170 (2004) 123–136.
[6] S.T. Hsu, K.T. Cheng, J.S. Chiou, Seawater desalination by direct contact membrane distillation, Desalination 143 (2002) 279–287.
[7] A. Larbot, L. Gazagnes, S. Krajewski, M. Bukowska, W. Kujawski, Water desalination using ceramic membrane distillation, Desalination 168 (2004) 367–372.
[8] A.E. Ghaly, M. Verma, Desalination of saline sludges using ion-exchange column with zeolite, Am. J. Environ. Sci. 4(4) (2008) 38–396.
[9] M.I. Occelli, H.H. Kessler (Eds.), Synthesis of Porous Materials: Zeolites, Clays and Nanostructures, CRC Press, New York, NY, 1997, pp. 44–46.
[10] R.M. Barrer, Hydrothermal Chemistry of Zeolites, Academic Press, New York, NY, 1982, pp. 20–21.
[11] B. Kwakye-Awuah, E. Von-Kiti, R. Buamah, I. Nkrumah, C. Williams, Effect of crystallization time on the hydrothermal synthesis of zeolites from kaolin and bauxite, Int. J. Sci. Eng. Res. 3(3) (2014) 1–7.
[12] B. Kwakye-Awuah, A. Mrozik, Z. Piotrowska-Seget, I. Nkrumah, C. Williams, I. Radecka, Release pattern of Ag^+ ions from silver-loaded zeolite X and its subsequent effect on fatty acid composition of bacterial cells, Int. J. Innov. Res. Technol. 2(11) (2013) 6235–12244.
[13] B. Kwakye-Awuah, E. Von-Kiti, I. Nkrumah, C. Williams, Towards the zeolitization of bauxite: Thermal behaviour of gibbsite in high-alumina-Ghanaian bauxite, Int. J. Eng. Res. Technol. 2(10) (2013) 1290–1300.
[14] B. Kwakye-Awuah, D.D. Wemegah, I. Nkrumah, C. Williams, I. Radecka, Antimicrobial activity of silver-zeolite lta on heavily-contaminated underground Ghanaian waters, Int. J. Sci. Res. (IJSR) 2(11) (2013) 26–31.
[15] B. Kwakye-Awuah, F.J.K. Adzabe, I. Nkrumah, C. Williams, Application of laboratory-synthesized ammonium zeolite LTX as soil amendment additive, Int. J. Sci. Basic Appl. Res. (IJSBAR) 12(1) (2013) 67–141.
[16] B. Kwakye-Awuah, L.K. Labik, I. Nkrumah, C. Williams, Removal of ammonium ion by laboratory-synthesized zeolite LTA adsorption from waters samples affected by mining activities in Ghana, J. Water Health 12(1) (2013) 151–160.
[17] B. Kwakye-Awuah, C. Williams, M.A. Kenward, I. Radecka, Antimicrobial action and efficiency of silver-loaded zeolite X, J. Appl. Microbiol. 104(5) (2008) 1516–1524.
[18] W. Mozgawa, The influence of some heavy metals cations on the FTIR spectra of zeolites, J. Mol. Struct. 555 (2000) 299–304.
[19] M.M. Treacy, J.B. Higgins, Collection of Simulated XRD Powder Patterns for Zeolites, Published on behalf of the Structure Commission of the International Zeolite Association, fourth revised ed., Elsevier, Amsterdam, 2001.
[20] A.R. García-Soto, G. Rodríguez-Niño, C.A. Trujillo, Zeolite LTA synthesis: Optimising synthesis conditions by using the modified sequential simplex method, Ing. Invest. 33(3) (2013) 22–27.
[21] E.M. Flanigen, R.L. Parton, R.L.W.P. Katonah, Silica polymorph and process for preparing same, C01B 33/12. 4073865, pp. 57–58.
[22] D. Coutinho, K. Balkus Jr., Preparation and characterization of zeolite X membranes via pulsed-laser deposition, Microporous Mesoporous Mater. 52(2) (2002) 79–91.

[23] D. Novembre, B.D. Sabatino, D. Gimeno, M. Garcia-Vallès, S. Martínez-Manent, Synthesis of Na–X zeolites from tripolaceous deposits (Crotone, Italy) and volcanic zeolitised rocks (Vico volcano, Italy), Microporous Mesoporous Mater. 75(1–2) (2004) 1–11.
[24] M. Kuronen, M. Weller, R. Townsend, R. Harjula, Ion exchange selectivity and structural changes in highly aluminous zeolites, React. Funct. Polym. 66(11) (2006) 1350–1361.
[25] F. Helffrich, Ion Exchange, Dower Publications, New York, NY, 1995, pp. 63–66.
[26] X. Guo, L. Zeng, X. Li, H.-S. Park, Ammonium and potassium removal for anaerobically digested wastewater using natural clinoptilolite followed by membrane pretreatment, J. Hazard. Mater. 151 (2008) 125–133.
[27] V.J. Inglezakis, A.A. Zorpas, M.D. Loizidou, H.P. Grigoropoulou, The effect of competitive cations and anions on ion exchange of heavy metals, Sep. Purif. Technol. 46(3) (2005) 202–207.
[28] J.D. Sherman, Ion exchange separations with molecular sieve zeolites, Zeolites: Sci. Technol. 80 (1984) 583–1123.
[29] B. Sefa-Ntiri, B. Kwakye-Awuah, C. Williams, Effect of zeolite types LTX and LTA on physicochemical parameters of drinking water samples in Ghana, assisted by light transmission experiment, Int. J. Res. Eng. Technol. 3(3) (2014) 1–7.
[30] D. Kučić, M. Markic, M. Briski, Ammonium adsorption on natural zeolite (clinoptilolite): Adsorption isotherms and kinetics modeling, Holistic Approach Environ. 2(4) (2012) 145–158.
[31] World Health Organization (WHO), Guidelines for Drinking-water Quality, third ed., 1(11), (2004), 45–196.